# Effects of ions on water structure: a low-field ¹H $T_1$ NMR relaxometry approach

## Pellegrino Conte*

**Aqueous salt solutions play an important role in nature because of their effects on environmental biogeochemical processes and on structural properties of biomolecules. Upon dissolution, salts split in ions that are solvated. Water in hydration shells is subjected to molecular motions that can be monitored by ¹H $T_1$ NMR relaxometry. This technique allowed the evaluation of the nature of the interactions between water and ions via variable temperature experiments. Examination of relaxometry properties of aqueous solutions at variable salt concentrations allowed acknowledgement of the role played by ions in either structuring or destructuring water aggregates. A mathematical model has been applied on six environmentally relevant salts: NaCl, KCl, $CaCl_2$, $CaCO_3$, $NaNO_3$, and $NH_4NO_3$. It was linear only for the concentration dependence of KCl-$R_1$. This model accorded with the one reported in literature where it has been considered valid only for diluted solutions. However, in the present study, the range of linearity for KCl was extended up to the saturation point. The model was modified for NaCl, $CaCl_2$, and $CaCO_3$ by using it as an exponential form in order to account for the nonlinearity of the $R_1$-versus-concentration curves. Nonlinearity was explained by the nonnegligible ion–ion interactions occurring as concentration was increased. Finally, further modification was needed to account for the asymmetric distribution of water around nitrate (in $NaNO_3$ and $NH_4NO_3$) and ammonium (in $NH_4NO_3$). This study is preliminary to the comprehension of the diffusion mechanisms of ions in water solutions at the equilibrium condition with solid surfaces such as soils and biochar-amended soils. Copyright © 2014 John Wiley & Sons, Ltd.**

**Keywords:** NMR; ¹H; $T_1$; relaxometry; fast field cycling; kosmotrope; chaotrope; water; salt solution

## Introduction

Ions in water play a very important role in many environmental biogeochemical processes and in influencing structural properties of biosystems (from the microscale up to the macroscale).[1–3] In environmental aqueous solutions (such as soils), ions are directly related to nutrition of living systems; to the electrochemical equilibriums and the redox potentials associated to environmental transformations (e.g. soil weathering);[4] to the conformations and activities of biomolecules;[5] to the regulation of the electrostatic potentials, conductance, and permeability of cell membranes;[6] and to the hydrophobic effect that drives partitioning, permeation, folding, and binding processes.[7]

Upon dissolution, salts are dissociated via solvation with water molecules. Two different hydration shells are usually identified.[8–11]

The innermost one is made by immobilized water (i.e. ice-like water) that is, in turn, surrounded by a second less ice-like shell (i.e. more random water) where water molecules are more disordered and mobile.[8–11] The third outermost water shell (generally indicated as bulk) can be also recognized when solutions are very diluted.[12] Here, water is less affected by the ionic field. In fact, the latter is weakened by the first two hydration shells and by the distance from the ion. The diffusional motion frequency of bulk water is larger than that in the most internal hydration shells.

The size of the hydration shells depends on both charge density and salt concentration. For diluted solutions, the larger the charge density, the thinner is the thickness of the hydration shells because of the strong effects of the electrical field generated by the ions.[8–11] In other words, water molecules lay closer to the ions. As salt concentration is increased, the space available for water in

the bulk progressively reduces, thereby making the presence of free moving water as solutions reach the saturation point impossible.[13] It must be also pointed out that water molecules in the innermost shells exchange with those in the outermost ones. The exchange rate is mediated by the charge density.[9] Namely, the larger the charge density, the slower is the exchange because of the higher capacity of ions to bind water molecules. Conversely, as charge density reduces, water mobility increases, and the exchange rate raises up.

Because of the aforementioned dissolution mechanism, the effects of ions on water organization (also referred to as water structure) in salt solutions can be monitored by analytical techniques sensitive to the timescale of water motions.[14] In particular, low-field nuclear magnetic resonance relaxometry with fast field cycling setup (FFC NMR) appears to be an innovative technique for these kinds of investigations.[15] In the classical instrumental arrangement, FFC NMR relaxometry allows the evaluation of the magnetic field dependence on the proton longitudinal relaxation times ($T_1$).

Proton longitudinal relaxation time values are affected by the strength of the dipolar interactions between a nucleus and its surroundings.[16] The stronger the dipolar interactions, the shorter are the $T_1$ values. Conversely, as dipolar interactions weaken, longer $T_1$ values are needed to achieve relaxation. Therefore, upon

* Correspondence to: Pellegrino Conte, Dipartimento di Scienze Agrarie e Forestali, Università degli Studi di Palermo, v.le delle Scienze edificio 4, 90128 – Palermo, Italy. E-mail: pellegrino.conte@unipa.it

Dipartimento di Scienze Agrarie e Forestali, Università degli Studi di Palermo, v.le delle Scienze edificio 4, 90128, Palermo, Italy

temperature variations, the frequency of molecular motions can be either reduced or raised because of freezing or warming conditions, respectively. In the first case, a strengthening of dipolar interactions is achieved, thus leading to $T_1$ reduction. In the latter, dipolar interactions are weakened and longer $T_1$ values are measured. However, it must be pointed out that the aforementioned mechanism, leading to the so-called fast motion regime (Fig. 1), explains the motional behavior of unconstrained liquid systems. Once a liquid is trapped between the walls of solid porous boundaries, a slow motion regime occurs (Fig. 1).[15,17] The weak interactions allowing adhesion of the liquid to the pore walls oppose the 3D exchange with the bulk liquid when temperature is increased.[15,17] For this reason, the liquid preferentially diffuses faster within the channels connecting pores between each other through a 2D motion. Because of the 2D diffusion, collision frequency with pore walls increases with temperature, thereby allowing an average residence time on pore walls longer than that retrieved at lower temperatures. As a consequence, shorter time for nuclei to relax is needed and lower $T_1$ values are achieved. Finally, the intermediate motion regime (Fig. 1) occurs when liquids containing relaxing nuclei are confined in soft matter (such as colloids). Here, temperature dependence of the molecular motions is affected not only by migration among relaxation sites having a distribution of surface-to-volume ratios but also by the skeletal movements of the soft matter.

According to the relaxation mechanisms depicted previously, it can be expected that water molecules in very diluted solutions are predominantly unconstrained, thereby accounting for a fast motion regime. On the other hand, as salt concentration is increased, water motion becomes progressively more restricted. For this reason, it can be expected that very concentrated salt solutions are subjected to a slow motion regime.[13,18]

The present study aims at the investigation of the nature of the interactions of water molecules around ions by applying $^1$H $T_1$ FFC NMR relaxometry at different temperatures and salt concentrations. In particular, environmentally relevant salts have been chosen: NaCl, KCl, $CaCl_2$, $CaCO_3$, $NaNO_3$, and $NH_4NO_3$. The arrangement of water around each ion has been evaluated, and mathematical models to predict water behavior around either simple or complex ions have
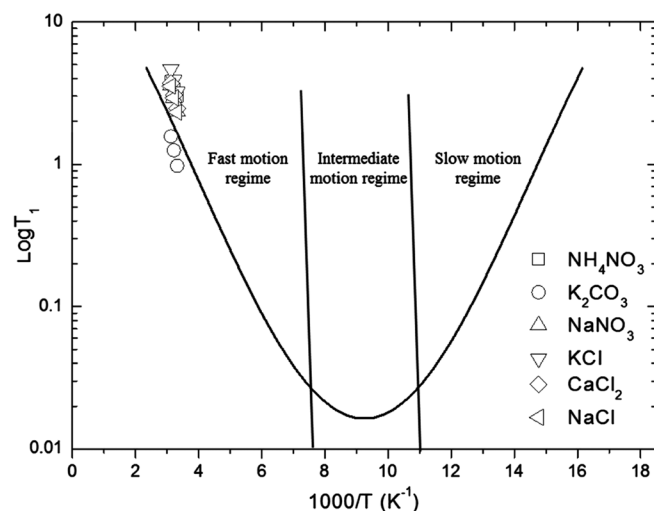
been achieved. The present study is the first step toward the understanding at the molecular level of the ion transport in environmental compartments when solid–liquid interfaces are present.

## Materials and methods

### Samples

Sodium chloride, potassium chloride, calcium chloride, sodium nitrate, ammonium nitrate, and potassium carbonate were all purchased from Sigma-Aldrich (Milan, Italy) and used without any preliminary treatment. All the salts were dissolved at different concentrations up to their saturation limit by using Milli-Q-grade water (resistivity 18.2 W, Merck-Millipore Simplicity 185, Milan, Italy). The solutions were degassed by an ultrasonic bath in order to remove the paramagnetic dissolved oxygen.

### $^1$H $T_1$ NMR relaxometry experiments

Salt solutions were analyzed by a Stelar Smartracer FFC Relaxometry instrument at a constant temperature of 28 °C. In order to verify whether the motion regime was fast, intermediate, or slow, experiments at 38 and 48 °C were also run.

The bases for the FFC NMR relaxometry have been already reported in Conte and Alonzo.[15] For this reason, only the experimental conditions applied for the present study are reported here. Namely, all the experiments have been conducted at the fixed relaxation field ($B_{RLX}$) of 2.5 mT. The period $\tau$, during which $B_{RLX}$ was applied, has been varied on 32 logarithmic spaced time sets. Thirty-two scans were set with a recycle delay (RD) of 60 s. A polarization field ($B_{POL}$) of 225 mT has been applied with a polarization time ($T_{POL}$) of 12 s. As experiments were conducted at 38 and 48 °C, $T_{POL}$ was fixed at 20 s and RD at 100 s. A $^1$H 90° pulse was applied at an acquisition field ($B_{ACQ}$) of 180 mT in order to retrieve the free induction decay with a time domain of 100 μs and 512 points. Field switching time was 3 ms, while spectrometer dead time was 15 μs.

### $^1$H $T_1$ NMR relaxometry data processing

The longitudinal relaxation time values ($T_1$) were achieved by interpolating the $^1$H magnetization recovery curves with the stretched exponential function (also known as Kohlraush–Williams–Watts function) reported in Eqn (1)[1] after exportation of the experimental data to OriginPro 7.5 SR6 (Version 7.5885, OriginLab Corporation, Northampton, MA, USA)[15]:

$$I(\tau) = I_0 \exp\left[ -\left( \frac{\tau}{T_1} \right)^k \right] + y_0 \qquad (1)$$

This equation provided the best fitting with the largest coefficients of determination ($R^2 > 0.998$). Equation (1) accounts for the large sample heterogeneity resulting in a multiexponential behavior of the recovery curves. In fact, this equation can be considered as a superposition of exponential contributions, thereby describing the likely physical picture of some distributions in $T_1$. Its application has the advantage that it is able to handle a wide range of relaxometry behaviors within only a single model. For this reason, assumptions about the number of exponentials to be used in modeling FFC NMR relaxometry data are not necessary.[15]

In Eqn (1), $I(\tau)$ is the $^1$H signal intensity at the $B_{RLX}$ value, $I_0$ is the $^1$H signal intensity at the thermal equilibrium, $T_1$ is the average



**Figure 1.** Thermal variation of the longitudinal relaxation time ($T_1$). The dots are the $T_1$ values of the salt solutions measured at 2.5 mT for temperature values of 28, 38, and 48 °C. The continuous line is the simulation of the temperature dependence of the dipolar proton longitudinal relaxation time as reported in reference.[16]

proton spin lattice relaxation time, $k$ is a heterogeneity parameter related to the stretching of the decay process, and $y_0$ is an offset parameter. All the measurements were performed at least in triplicate.

## Results and discussion

### The motion regime of the salt solutions

Figure 1 shows the simulation (continuous line) of the evolution of the longitudinal relaxation time values ($T_1$) versus the temperature. This behavior appears as a V-shaped curve because of the Lorentzian form of the spectral density function describing the distribution of the motion frequencies (and therefore dipolar interactions) in a molecular system.[15] The meaning of the three motion regimes in Fig. 1 has been already reported in the Introduction.

The salts used in the present study were dissolved at different concentrations up to the saturation point and the $T_1$ values measured at three different temperatures as indicated in Materials and Methods. The data points reported in Fig. 1 show an increment of the longitudinal relaxation times of the saturated solutions as temperature was raised up (right to left in Fig. 1). The diluted solutions revealed the same trend and thus are not reported.

Regardless of their concentration, all the salt solutions revealed fast motion regime. The latter can be explained by considering that, in the absence of paramagnetic species, the overall longitudinal relaxation time is inversely modulated by two factors.[15,18,19] The first one is the mean residence lifetime of the bound water that is also referred to as exchange time (ET). This is the time during which water molecules lay in the ice-like hydration shell. The faster the exchange rate among water molecules from the innermost hydration shell to the outermost ones, the shorter is the ET value. Conversely, as water molecules stay longer in the ice-like layer, the exchange rate among hydration shells slackens, thereby providing longer ET values.

The second factor accounting for the motion regime of aqueous solutions is the time needed for the longitudinal relaxation of the bound water. This time is related to the strength of the dipolar interactions among water molecules in the ice-like shell and those belonging to the outermost ones. Namely, the weaker the dipolar interaction strengths, the longer is the time needed for proton relaxation.

Following temperature enhancement, molecular mobility increases. As a consequence, the ET shortens, while the longitudinal relaxation time of the bound water lengthens. When the former time becomes negligible as compared with the latter one, the fast motion regime occurs and the overall longitudinal relaxation time results inversely related to the temperature variations as showed by the experimental dots in Fig. 1.

According to Arrhenius equation,[15,16] the slopes retrieved from the linear regressions of the Log($T_1$)-versus-1000/$T$ curves (Fig. 1) provide the activation energy ($E_a$) values of the water molecular motions.[15,16] Table 1 shows that the $E_a$ values for some selected salt concentrations are similar to each other, thereby confirming that the nature of the ion–water interactions is independent of the nature of the salt. In particular, the electron-deficient cations interact with the electron-rich oxygen atom in water via electrostatic interactions. On the other hand, the electron-rich anions interact with the electropositive hydrogen atoms in water through formation of pseudo-H bonds (i.e. H bridges between the anions in solution and the oxygen in water).[20] Both kinds of interactions are dipolar in nature. Moreover, the stronger the ion–water interactions, the stronger polarization degree of the water molecules in the ice-like shell results. This leads toward stronger H bonds with

**Table 1.** Activation energy value ($E_a$) needed to trigger the molecular motions of water in the salt solutions

| Salts | Concentration | $E_a$ |
|---|---|---|
| | mol L$^{-1}$ | kJ mol$^{-1}$ |
| KCl | 1.0 | 15.4 ± 0.1 |
| | 2.0 | 15.3 ± 0.2 |
| | 3.0 | 14.6 ± 0.2 |
| NaCl | 3.0 | 15.4 ± 0.3 |
| | 4.0 | 16.8 ± 0.2 |
| | 5.0 | 17.0 ± 0.5 |
| NaNO$_3$ | 3.0 | 15.2 ± 0.1 |
| | 5.0 | 16.0 ± 0.2 |
| | 6.0 | 17.1 ± 0.2 |
| CaCl$_2$ | 0.4 | 15.3 ± 0.2 |
| | 1.5 | 16.0 ± 0.1 |
| | 2.0 | 16.3 ± 0.2 |
| K$_2$CO$_3$ | 0.4 | 16.6 ± 0.4 |
| | 1.0 | 15.3 ± 0.7 |
| | 5.0 | 19.2 ± 0.5 |
| NH$_4$NO$_3$ | 1.0 | 16.4 ± 0.3 |
| | 3.0 | 14.1 ± 0.3 |
| | 5.0 | 12.6 ± 0.1 |
| | 6.0 | 10.8 ± 0.2 |
| | 8.0 | 9.8 ± 0.3 |
| | 10.0 | 9.4 ± 0.2 |

The table shows $E_a$ values only for some of the concentrations used in the present study.

the water molecules included within the outermost hydration shells. Conversely, weakening of the ion–water interactions induces weaker H bonds with water in the outermost hydration layers.

According to the H-bond strength among water molecules, water motion activation may require different amounts of energy. Table 1 shows that the $E_a$ value increases when the concentration of sodium chloride, calcium chloride, sodium nitrate, and potassium carbonate is raised up. Conversely, reduction of activation energy is retrieved when the concentration of potassium chloride and ammonium nitrate is increased. In order to explain such a behavior, the role of ions on water structure must be accounted for (refer to discussion in the succeeding texts).

### Qualitative evaluation of the structure maker and structure breaker activity of ions in aqueous solutions

Salt dissolution in water involves formation of three hydration shells. The strong ionic fields force the nearby polar water molecules to be ordered, thereby pulling them away from their H-bond configuration.[11,20,21] In particular, high-density-charge cations have two effects. On the one hand, the electron-deficient cations interact with the oxygen in water. For this reason, formation of a rigid ice-like shell, which is not flexible enough to sustain H bonds among water molecules in the first hydration layer, occurs. On the other hand, the strong electrostatic interactions induce high polarization of the oxygen atoms in the water molecules coordinated to the metal ions. As a consequence, formation of stronger hydrogen bonds with adjacent water molecules in the second hydration shell is achieved.[22] As the distance from the ions increases, the effect of the ionic fields decreases, and water molecules regain their normal behavior (i.e. they behave as a bulk). The aforementioned effects

apply also to high-density-charge anions. The sole difference lies in the orientation of water around anions. In fact, the electron-rich anions interact with the electropositive hydrogen atoms through formation of pseudo-H bonds.

Ions (either cations or anions) that are able to break the H-bond network among water molecules in the first hydration shell, thus favoring an ordered ice-like structure, are regarded as structure makers or kosmotropes.[22]

Upon charge density reduction, decrement of the electrostatic force between ions and surrounding water occurs. This leads to stronger water–water H bonds in the first hydration shell. As a consequence, less ice-like structured water is retrieved. In addition, H bonds between water molecules in the first and in the outermost hydration shells are weaker than in the case of high-charge-density ions. Again, as the distance from the ions increases, water molecules regain their normal behavior, thus behaving as a bulk.

All the ions (either cations or anions) incapable to disrupt the H-bond network among water molecules in the first hydration shell, thus leading to a less ice-like structure, are indicated as structure breakers or chaotropes.[22]

Once water molecules turn more rigid because of the kosmotropic action of the ions in aqueous solutions, a shortening of the $T_1$ values must be expected. In fact, as aforementioned, enhancement of water molecular rigidity in the first hydration shell induces stronger H bonds with the water molecules in the surrounding more external hydration layers. For this reason, an increase of the intermolecular dipolar interactions occurs, thereby producing shorter proton longitudinal relaxation times. Conversely, as ionic chaotropic action befalls, $T_1$ values are expected to be longer. In fact, the weak electrostatic interactions between ions and the first hydration layer water molecules are unable to strengthen the interlayer H bonds. The consequences are dipolar interactions weaker than in the previous case and hence longer time for longitudinal relaxation.[12,23,24]

Because of the inverse relationship between longitudinal relaxation time and longitudinal relaxation rate (i.e. $T_1 = 1/R_1$), the kosmotropic action of ions on water structure produces faster $R_1$ values, whereas chaotropic action provides slower $R_1$ values.[12]

According to the aforementioned mechanism, the increment of $R_1$ values *versus* salt concentration reveals that sodium chloride, calcium chloride, and potassium carbonate have a kosmotropic action on water structure (Fig. 2). This behavior can be accounted for by considering that sodium, calcium, and carbonate ions are structure makers.[11,22,25,26] Conversely, chloride shows a weak structure breaker action,[22] while potassium is regarded either as being almost neutral in its effects on water structure[11] or as being a weak chaotrope.[24] For this reason, it can be argued that, as salt concentration increases, the kosmotropic actions of sodium and calcium ions predominate over the weak chaotropic effect of chloride ion. This leads to the increment of the $R_1$ values observed for the NaCl and CaCl$_2$ solutions (Fig. 2). Finally, because of the almost neutral or weak chaotropic effects of potassium on water structure,[11] only the strong kosmotropic action of carbonate ion may account for the $R_1$ behavior of K$_2$CO$_3$ solutions in Fig. 2.

It is noteworthy that the $R_1$-versus-concentration curves for the solutions of calcium chloride and potassium carbonate range in wider intervals than those retrieved for the solutions containing sodium chloride (Fig. 2). In fact, while $R_1$ values of NaCl solutions range between 0.34 and 0.44 s$^{-1}$ (Fig. 2), those measured for CaCl$_2$ and K$_2$CO$_3$ solutions are in the 0.34–1.1-s$^{-1}$ interval (Fig. 2). The explanation for such a behavior is related to the polyvalent nature of calcium and carbonate. In fact, the larger the ionic charge, the

stronger the ionic kosmotropic action is.[11,12,22–25] In other words, the interlayer H bonds induced by Ca$^{2+}$ and CO$_3^{2-}$ are stronger than those induced by Na$^+$, thereby providing faster proton longitudinal relaxation rate values.

Further evidence for NaCl, CaCl$_2$, and K$_2$CO$_3$ kosmotropic effect lies in the $E_a$ values reported in Table 1. In fact, as already indicated in the previous paragraph, the activation energy for water molecular motion increases as the amount of sodium chloride, calcium chloride, and potassium carbonate is raised (Table 1). The larger the amount of kosmotropes in solution, the stronger the electrostatic interactions that promote higher polarization of the atoms in the water molecules coordinated to the ions are (i.e. oxygen in the case of cations and hydrogen in the case of anions). For this reason, formation of stronger hydrogen bonds between water molecules belonging to adjacent hydration shells is achieved.[22] Once the strength of H bonds is enhanced, the activation of water molecular motions requires higher $E_a$ values (Table 1).

Figure 2 shows a linear variation of the longitudinal relaxation rate for water molecules interacting with different concentrations of KCl, a weak V-shaped curve for NaNO$_3$, and a well-defined V-shaped curve for the $R_1$ values measured at increasing amounts of NH$_4$NO$_3$.

As aforementioned, chloride is a weak structure breaker,[22] whereas potassium appears either to have no effects[11] on water structure or to have a weak structure breaker property.[24] The predominance of the weak chaotropic activities explains the reduction of $R_1$ as KCl concentration is increased. In fact, chaotropic ions are able to strengthen intermolecular H bonds among water molecules in the first hydration shell.[22] As a consequence, intershell hydrogen bonds weaken. The larger the amount of chaotropes, the weaker the intershell H-bonds are, thereby providing weaker dipolar interactions and slower $R_1$ values (decreasing linear trend in Fig. 2 for KCl). Because of the progressive reduction of the intershell hydrogen bond strength, lower $E_a$ values are retrieved as reported in Table 1.

Sodium and ammonium nitrate salts are made by ions with a contrasting action for water structure. In fact, sodium and ammonium are structure makers, whereas nitrate shows a structure breaker activity.[25,26] The V-shaped trends for NaNO$_3$ and NH$_4$NO$_3$ solutions (Fig. 2) can be accounted for by hypothesizing that the chaotropic action of nitrate ion prevails up to the concentration of *ca* 1 and 5 mol l$^{-1}$, respectively. Above the aforementioned limits, the kosmotropic actions of sodium and ammonium ions predominate. According to the hypothesis on the role played by sodium, ammonium, and nitrate ions in different concentration intervals, a V-shaped trend is expected also for the $E_a$ values reported in Table 1. Conversely, Table 1 shows an increment of NaNO$_3$ $E_a$ values and a reduction of NH$_4$NO$_3$ $E_a$ values up to the saturation. At the moment, there is no valid explanation for such a diametric behavior.

## Quantitative aspects of kosmotropic and chaotropic actions of ions in aqueous solutions

### $R_1$-versus-KCl concentration

Youshida *et al.*[24] reported that, for diluted solutions, salt concentration dependence of the longitudinal relaxation rate keeps the linearity according to Eqn (2):

$$\frac{R_1}{R_1^0} = 1 + Bm \tag{2}$$

Here, $R_1$ is the longitudinal relaxation rate of the solution, $R_1^0$ is the longitudinal relaxation rate of the pure solvent, $m$ is the molality (mol kg$^{-1}$), and $B$ is a coefficient determined by the experiment. The latter parameter reflects the strength of the ion–solvent interactions and is usually considered as the sum of the contribution of each ion in solution (i.e. $B = B^+ + B^-$). The lower the $B$ value, the stronger the chaotropic action is. Conversely, as the $B$ value increases, kosmotropic action prevails. Because of the direct relationship between molality and molarity (M, mol l$^{-1}$), in the present study, the latter has been used instead of the former in Eqn (2).

Figure 2 shows that the linear condition given by Eqn (2) is satisfied only by potassium chloride. Surprisingly, linearity was applied up to KCl saturation point. This can be accounted for by the nature of the longitudinal relaxation rates measured in the present study. In fact, here, low-field $^1H$ NMR relaxometry experiments have been conducted, whereas Youshida et al.[24] performed high-field $^{17}O$ NMR relaxometry experiments. While $^{17}O$ NMR measurements are affected only by water dynamics (i.e. molecular rotations and translations), proton relaxometry behavior is affected also by water chemical exchange phenomena (i.e. dynamic H bonds). For this reason, sensitivity lack, as a result of both application of low magnetic field and fast chemical exchanges, can affect $R_1$ measurements in the present study, thereby allowing longitudinal relaxation rate linearity over a wider range of KCl concentrations. Notwithstanding the different experimental settings, application of the condition $B^+ = B^-$ (i.e. the $B$ contributions for K$^+$ and Cl$^-$ were considered identical) in order to fit KCl data in Fig. 2 by Eqn (2)[24] provided K$^+$ and Cl$^-$ $B$ values of $-0.019 \pm 0.001$ (Table 2). These findings accord to those reported in Youshida et al.[24]

(i.e. $B^+ = B^- = -0.017$), thus supporting the validity of the application of the linear model also on $^1H$ NMR relaxometry measurements performed in low-field conditions. Moreover, the small negative $B^+$ and $B^-$ values for K$^+$ and Cl$^-$, respectively, confirm the weak chaotropic nature of both ions as previously indicated.

### $R_1$-versus-NaCl/K$_2$CO$_3$/CaCl$_2$ concentration

Deviations from linearity as a result of the nonnegligible interion interactions as concentration increases have been observed in NaCl, CaCl$_2$, and K$_2$CO$_3$ solutions (Fig. 2). In order to account for the nonlinearity of the experimental data, Eqn (2) has been rewritten as Eqn (3) by considering that the former is the approximation to the linear part of the Taylor series expansion of the latter:

$$\frac{R_1}{R_1^0} = \exp[(B^+ + B^-)M] \quad (3)$$

The fitting of the experimental data has been run by using as a sole constraint $B^+ = B^- = -0.019 \pm 0.001$ as evaluated previously. The $R_1^0$ value of pure water as well as the $B$ parameters for each ion has been reported in Table 2. The $R_1^0$ values accord to that experimentally retrieved within the experimental error limits, while the coefficient of correlations ($R^2$) for each fitting curve were all above 0.98, thereby providing the first support to the validity of the model depicted in Eqn (3). Further support comes from the $B$ coefficients of sodium and carbonate ions obtained by NaCl and K$_2$CO$_3$ solutions, respectively (Table 2). In particular, the sodium $B^+$ coefficient
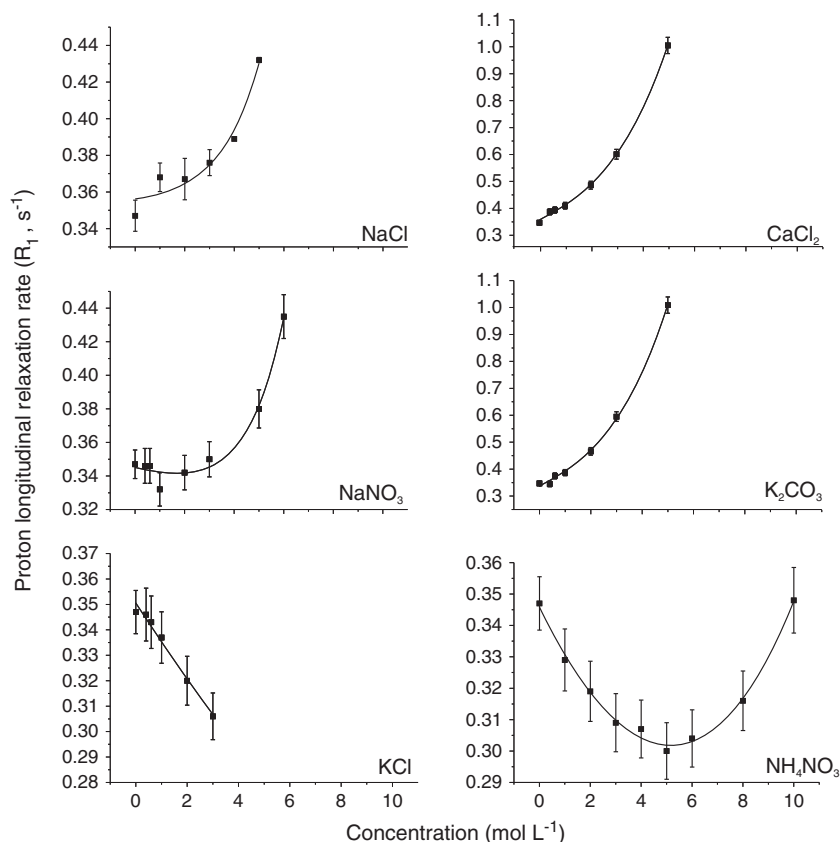


**Figure 2.** Longitudinal relaxation rate ($R_1$) dependence upon concentration in mol l$^{-1}$ of solutions containing sodium chloride, sodium nitrate, calcium chloride, potassium carbonate, potassium chloride, and ammonium nitrate.

resulted in 0.057 ± 0.008 (Table 2), which is in good agreement with that reported in Youshida et al.[24] (i.e. 0.053). The carbonate $B^-$ coefficient was 0.25 ± 0.01 (Table 2) similar to that indicated in dos Santos et al.[27] (i.e. 0.294).

It must be noticed that the $B$ coefficient for sodium ion obtained in the present study and in Youshida et al.[24] and the $B$ coefficient for carbonate ion obtained here were lower than those reported in dos Santos et al.[27] (i.e. 0.085 for sodium and 0.294 for carbonate ion, respectively). The latter discrepancy can be attributed to the techniques applied to retrieve $B$ coefficients. In fact, NMR relaxometry techniques have been applied here and in Youshida et al.,[24] whereas viscosimetry measurements have been used in dos Santos et al.[27]

Finally, application of Eqn (3) to fit the data points of CaCl$_2$ solutions (Fig. 2) revealed a $Ca^{2+}$ $B$ coefficient of 0.24 ± 0.01 (Table 2), which is similar to that reported in Afzal et al.[28] (i.e. 0.2071). Once again, the discrepancy between the $B$ coefficient measured in the present study and that reported in Afzal et al.[28] can be attributed to the differences between the NMR relaxometry technique used here and the viscosimetry evaluations applied in Afzal et al.[28]

It is worth noting that the $B$ coefficients reported in Table 2 reflect the kosmotropic/chaotropic action of each ion as qualitatively indicated in the previous paragraph. Namely, the $B$ trend for the cation kosmotropic action is $Ca^{2+} > Na^+ > K^+$, whereas that for anions is $CO_3^{2-} > Cl^-$ (obviously, the $B$ trend for chaotropic actions is the opposite). As aforementioned, both series can be accounted for by the differences in the ionic charge densities that follow the same trend.[9] In fact, the larger the ionic charge density, the stronger the kosmotropic action of the ions is. Conversely, as ionic charge density reduces, chaotropic action prevails.

### $R_1$-versus-NaNO$_3$/NH$_4$NO$_3$ concentration

Equation (3) did not apply to fit the experimental data for nitrate salts reported in Fig. 2. According to the quantum mechanical calculations reported in Salvador et al.,[29] the solvated planar nitrate in $[NO_3(H_2O)_n]^-$ clusters binds water molecules to form an asymmetric hydration shell where nitrate prefers a surface rather than an interior location in the water pod. The asymmetrical water displacement produces a distribution of H bonds having different lengths and strengths. For this reason, a distribution of water interhydration–shell exchange motions is conceivable.

Equation (3) has been rewritten as Eqn (4) in order to account for the nonlinearity of the NaNO$_3$/NH$_4$NO$_3$ R$_1$-versus-concentration graphs in Fig. 2, attributable to the asymmetry of the first hydration shell around nitrate anion.

$$R_1 = R_1^1 \exp\left[(B_1^+ + B_1^-)M\right] + R_1^2 \exp\left[(B_1^+ + B_2^-)M\right] \quad (4)$$

The two terms in Eqn (4) describe the proton longitudinal relaxation rate of two different water types. They differ between each other only in the way that they are bound to the nitrate anion within the $[NO_3(H_2O)_n]^-$ clusters. In particular, Eqn (4) is based on the hypothesis that only two types of different H bonds (i.e. a weak and a strong H bond) are involved in the interactions with the anion. Each water molecule may interact with the nitrate anion only through one of these bonds: either by strong or by weak H bond. The assumptions on the number of H bonds involved in the water–nitrate interactions have been chosen in order to prevent that the number of parameters in the fitting procedure could be larger than the experimental data points. The latter were eight for NaNO$_3$ and nine for NH$_4$NO$_3$ (Fig. 2). The fitting parameters in Eqn (4) are $R_1^1$, the proton longitudinal relaxation rate of the first

**Table 2.** Mathematical models applied to fit the experimental data reported in Fig. 2

| Sample | Mathematical model | $R_1^0$ (s$^{-1}$) | | $B^-$ (l mol$^{-1}$) | | $B^+$ (l mol$^{-1}$) | |
|---|---|---|---|---|---|---|---|
| KCl | $\frac{R_1}{R_1^0} = 1 + (B^+ + B^-)M$ | 0.347 ± 0.008[a] | | −0.019 ± 0.001[b] | | −0.019 ± 0.001[b] | |
| NaCl | $\frac{R_1}{R_1^0} = \exp[(B^+ + B^-)M]$ | 0.347 ± 0.009[b] | | −0.019 ± 0.001 | | 0.057 ± 0.008[b] | |
| K$_2$CO$_3$ | $\frac{R_1}{R_1^0} = \exp[(B^+ + B^-)M]$ | 0.31 ± 0.01[b] | | 0.25 ± 0.01[b] | | −0.019 ± 0.001 | |
| CaCl$_2$ | $\frac{R_1}{R_1^0} = \exp[(B^+ + B^-)M]$ | 0.33 ± 0.01[b] | | −0.019 ± 0.001 | | 0.24 ± 0.01[b] | |
| | | $R_1^1$ (s$^{-1}$) | $R_1^2$ (s$^{-1}$) | $B_1^+$ (l mol$^{-1}$) | $B_1^-$ (l mol$^{-1}$) | $B_1^+$ (l mol$^{-1}$) | $B_2^-$ (l mol$^{-1}$) |
| NaNO$_3$ | $R_1 = R_1^1 \exp[(B_1^+ + B_1^-)M] + R_1^2 \exp[(B_1^+ + B_2^-)M]$ | $2.8 \pm 0.1 \times 10^{-3}$ | 0.34 ± 0.02 | 0.057 ± 0.008 | 0.6 ± 0.2[b] | 0.6 ± 0.2[b] | −0.072 ± 0.002[b] |
| | | $R_1^1$ (s$^{-1}$) | $R_1^2$ (s$^{-1}$) | $B_1^+$ (l mol$^{-1}$) | $B_2^+$ (l mol$^{-1}$) | $B_1^+$ (l mol$^{-1}$) | $B_2^-$ (l mol$^{-1}$) |
| NH$_4$NO$_3$ | $R_1 = R_1^1 \exp[(B_1^+ + B_1^-)M] + R_1^2 \exp[(B_2^+ + B_2^-)M]$ | $56 \pm 2 \times 10^{-3}$ | 0.29 ± 0.02 | −0.65 ± 0.02[b] | 0.21 ± 0.03[b] | 0.6 ± 0.2 | −0.072 ± 0.002 |

$B^+$ and $B^-$ are the fitting parameters describing the kosmotropic and chaotropic actions of cations and anions, respectively. For sodium nitrate and ammonium nitrate, a separation between the kosmotropic and chaotropic contributions of cations and anions was impossible. $R_1^0$ is the proton longitudinal relaxation time of deionized water.
a. $R_1^0$ value of pure water. The error has been obtained by three replicates.
b. Obtained by the application of the mathematical model. The error is from the fitting procedure.

kind of water molecule; $R_1^2$, the proton longitudinal relaxation rate of the second kind of water molecule; $B_1^+$, the coefficient describing the strength of the interactions between water and cations; $B_1^-$, the coefficient describing the strength of the first type of nitrate–water interactions; and $B_2^-$, the coefficient describing the strength of the second type of nitrate–water interactions.

Equation (4) was run to fit NaNO$_3$ experimental data (Fig. 2) by using the Na$^+$ $B$ coefficient retrieved for NaCl (Table 2) as a constraint. The fitting returned a coefficient of correlation of 0.97 and $R_1^1$ and $R_1^2$ values that, summed, produced a value of 0.34 $\pm 0.02$ s$^{-1}$. The latter corresponds to the experimental $R_1^0$ measured for pure water (i.e. $0.347 \pm 0.008$ s$^{-1}$), thereby confirming that Eqn (4) provides the longitudinal relaxation rate of pure water as salt concentration is null. $B_1^-$ and $B_2^-$ values resulted in $0.6 \pm 0.2$ and $-0.072 \pm 0.002$ l mol$^{-1}$, respectively (Table 2). The positive $B_1^-$ value is an indication that nitrate acts as a kosmotrope (i.e. it strongly binds some water molecules, thus acting as a structure maker), whereas the negative $B_2^-$ value indicates a chaotropic action of the anion (i.e. nitrate is weakly bound to some other water molecules, thus acting as a structure breaker). This diametrical behavior of nitrate anion for what concerns its action on water structure appears to confirm the quantum mechanical calculations provided by Vchirawongkwin et al.[26] In fact, the authors concluded that 'the mean residence time for water ligands in general classify [...] nitrate as a moderate and weak structure making anion, while the specific values for individual sites of nitrate reveal local weak structure breaking properties'.

The attempts to apply Eqn (4) to fit NH$_4$NO$_3$ data reported in Fig. 2 by using as constraints the nitrate $B_1^-$ and $B_2^-$ values obtained previously completely failed. A possible explanation for this failure may lie in the nature of the solvation shell around ammonium ion. In fact, quantum mechanical calculations revealed that ammonium binds up to five water molecules in the first hydration shell.[30] Four molecules form a long-lived tetrahedral cage around the cation. Each of the four water molecules is hydrogen bonded with one proton of NH$_4^+$. The fifth molecule is more mobile and may exchange with one of the four molecules in the tetrahedral cage. Because two differently bound water molecules can be recognized in the ammonium hydration shell, it is possible to argue that, as for nitrate anion, the $B$ coefficient for this cation must be split in two components as indicated in Eqn (5). The first $B_1^+$ component is associated to the motion-restrained water molecules, whereas the second $B_2^+$ component is related to the relatively free moving molecule.

$$R_1 = R_1^1 \exp\left[\left(B_1^+ + B_1^-\right)M\right] + R_1^2 \exp\left[\left(B_2^+ + B_2^-\right)M\right] \quad (5)$$

The fitting procedure performed on the data points of ammonium nitrate provided the fitting curve reported in Fig. 2 ($B_1^-$ and $B_2^-$ values for nitrate anion were used as constraints with the values of $0.6 \pm 0.2$ and $-0.072 \pm 0.002$ l mol$^{-1}$, respectively). The coefficient of correlation was 0.99, while the $R_1^1$ and $R_1^1$ values returned the sum of $0.35 \pm 0.02$ s$^{-1}$, which is similar to the experimental $R_1^0$ measured for pure water. As for Eqn (4), it can be concluded that also Eqn (5) provides the experimental value of the longitudinal relaxation rate of pure water as salt concentration is null.

The numerical values for $B_1^+$ and $B_2^+$ were $-0.65 \pm 0.02$ and $0.21 \pm 0.03$, respectively. The negative $B_1^+$ value indicates ammonium cation as a chaotrope. This can be explained by the presence in the hydration shell of the more mobile water molecule described previously.[30] In fact, the weak bonding of water to the cation may induce weaker H bonds with the water molecules in the outermost shells, thereby leading to a less structured water system

(chaotropic effect). The positive $B_2^+$ value indicates ammonium cation as a kosmotrope. In fact, the water molecules strongly hydrogen bonded to ammonium as described previously[30] result more polarized than normal because of the strong interaction with the cation. As a consequence, water in the first hydration shell around ammonium can form stronger H bonds with water molecules in the outermost shells, thus leading to a more structured water system (kosmotropic effect).

## Conclusions

This study reports for the first time a low-field $^1$H $T_1$ NMR relaxometry approach to understand the behavior of water in salt solutions. Results qualitatively revealed that sodium chloride, calcium chloride, and potassium carbonate act as kosmotropes, whereas chaotropic action of potassium chloride has been recognized. Sodium and ammonium nitrate salts acted as both kosmotropes and chaotropes according to the range of salt concentration within which the structure making and structure breaking nature of cations and anions predominates.

The quantitative evaluation of the kosmotropic/chaotropic effect of ions showed that the $B$ coefficients were in the order Ca$^{2+}$ > Na$^+$ > K$^+$ for cations and CO$_3^{2-}$ > Cl$^-$ for anions, thereby confirming that charge density is directly responsible for the strength of the ion–water interactions.[8–11] However, as the structure of the ions turned more complex (such as in nitrate and ammonium), a dual action, attributable to the asymmetric distribution of water in the hydration shells, was identified. In particular, two different kinds of water molecules were hypothesized around ammonium and nitrate. The first water type is strongly bound to the ions, whereas the second type is more mobile and hence weakly interacting either with nitrate or with ammonium. The strong ion–water interactions induce water structuring, thereby leading to the kosmotropic action. Conversely, as water weakly interacts with the ions, the chaotropic action occurs.

Although carbonate shows the same complexity as nitrate, it did not reveal the kosmotropic/chaotropic duality. This is probably because of the symmetry of the water hydration shell as the anion is placed in solution.

Acknowledgement of the water–ion interactions in salty solutions is very crucial to explain the nutrient transport mechanisms in environmentally relevant porous materials, such as soils and biochar. In fact, as an example, it is still unclear how biochar may affect soil nutrient availability to plants or microbes when it is applied to soils. Are the kosmotropic and chaotropic ion actions involved in the affinity of biochar for anions and cations? Are the aforementioned effects implicated in nutrient leaching in biochar-amended soils? Is it possible to achieve biochars that selectively adsorb/desorb mineral nutrients as they are needed for plant nutrition? Further studies are hence still needed in order to answer the questions in the preceding texts, thereby making the results reported in the present study preparatory to those aims.

## References

[1] R. E. White, *Principle and practices of soil science*, Blackwell Publishing, Oxford, UK, **2006**.

[2] K. H. Tan, *Principles of soil chemistry*, 4th edn, CRC Press Taylor & Francis Group, Boca Radon, FL (USA), **2011**.

[3] C. De Duve, *Singularities, landmarks in the pathway to life*, Cambridge University Press, NY (USA), **2005**.

[4] K. H. Tan, *Handbook of Processes and Modelling in the Soil-Plant System*, The Hartworth Press Inc., Binghamton NY (USA), **2003**, pp. 27–56.

[5] D. L. Beauchamp, M. Khajehpour. *Biophys. Chem.* **2012**, *161*, 29–38.

[6] R. Munns. *Plant Cell Environ.* **2002**, *25*, 239–250.

[7] J. N. Israelachvili, *Intermolecular and surface forces*, Academic Press, London, UK, **1992**.

[8] Y. Marcus. *Pure Appl. Chem.* **1987**, *59*(8), 1093–1101.

[9] Y. Marcus. *Chem. Rev.* **1988**, *88*, 1475–1498.

[10] C. W. Bock, G. D. Markham, A. K. Katz. *Theor. Chem. Acc.* **2006**, *115*, 100–112.

[11] A. K. Soper, K. Weckström. *Biophys. Chem.* **2006**, *124*, 180–191.

[12] T. H. Plumridge, R. D. Waigh. *J. Pharm. Pharmacol.* **2002**, *54*, 1155–1179.

[13] Y. Marcus. *J. Solution Chem.* **2009**, *38*, 513–516.

[14] M. H. Levitt, *Spin Dynamics*, Wiley, Chichester, England, **2008**.

[15] P. Conte, G. Alonzo. *eMagRes* **2013**, *2*, 389–398.

[16] V. I. Bakhmutov, *Practical NMR relaxation for chemists*, John Wiley and Sons Ltd., Chichester, West Sussex, England, **2004**.

[17] P. Conte, U. M. Hanke, V. Marsala, G. Cimò, G. Alonzo, B. Glaser. *J. Agric. Food Chem.* **2014**, *62*, 4917−4923.

[18] R. B. Lauffer. *Chem. Rev.* **1987**, *87*, 901–927.

[19] S. Laurent, D. Forge, M. Port, A. Roch, C. Robic, L. V. Elst, R. N. Muller. *Chem. Rev.* **2008**, *108*, 2064–2110.

[20] P. Lo Nostro, B. W. Ninham. *Chem. Rev.* **2012**, *112*, 2286–2322.

[21] B. Hribar, N. T. Southall, V. Vlachy, K. A. Dill. *J. Am. Chem. Soc.* **2002**, *124*, 12302–12311.

[22] H. Kanno, K. Yonehama, A. Somraj, Y. Yoshimura. *Chem. Phy. Lett.* **2006**, *427*, 82–86.

[23] A. Geiger, H. G. Hertz. *J. Solution Chem.* **1976**, *5*(6), 365–388.

[24] K. Youshida, K. Ibuki, M. Ueno. *J. Solution Chem.* **1996**, *25*(5), 435–453.

[25] J. R. C. van der Maarel, D. Lankhorst, J. de Bleijser, J. C. Leyte. *J. Phys. Chem.* **1986**, *90*, 1470–1478.

[26] V. Vchirawongkwin, C. Kritayakornupong, A. Tongraar, B. M. Rode. *J. Phys. Chem. B* **2011**, *115*, 12527–12536.

[27] A. P. dos Santos, A. Diehl, Y. Levin. *Langmuir* **2010**, *26*, 10778–10783.

[28] M. Afzal, M. Saleem, M. T. Mahmood. *J. Chem. Eng. Data* **1989**, *34*, 339–346.

[29] P. Salvador, J. E. Curtis, D. J. Tobias, P. Jungwirth. *Phys. Chem. Chem. Phys.* **2003**, *5*, 3752–3757.

[30] F. Brugé, M. Bernasconi, M. Parrinello. *J. Am. Chem. Soc.* **1999**, *121*, 10883–10888.